OXFORD

Whole-brain connectivity during encoding: age-related differences and associations with cognitive and brain structural decline

Elettra Capogna [1],*, Markus H. Sneve [1], Liisa Raud[1], Line Folvik[1], Hedda T. Ness [1], Kristine B. Walhovd [1,2], Anders M. Fjell[1,2], Didac Vidal-Piñeiro[1]

[1]Centre for Lifespan Changes in Brain and Cognition, Department of Psychology, University of Oslo, 0373 Oslo, Norway,
[2]Department of Radiology and Nuclear Medicine, Oslo University Hospital, 0424 Oslo, Norway
*Corresponding author: Department of Psychology, University of Oslo, 0317 Oslo, Norway. Email: elettra.capogna@psykologi.uio.no

There is a limited understanding of age differences in functional connectivity during memory encoding. In the present study, a sample of cognitively healthy adult participants ($n = 488$, 18–81 years), a subsample of whom had longitudinal cognitive and brain structural data spanning on average 8 years back, underwent functional magnetic resonance imaging while performing an associative memory encoding task. We investigated (1) age-related differences in whole-brain connectivity during memory encoding; (2) whether encoding connectivity patterns overlapped with the activity signatures of specific cognitive processes, and (3) whether connectivity associated with memory encoding related to longitudinal brain structural and cognitive changes. Age was associated with lower intranetwork connectivity among cortical networks and higher internetwork connectivity between networks supporting higher level cognitive functions and unimodal and attentional areas during encoding. Task-connectivity between mediotemporal and posterior parietal regions—which overlapped with areas involved in mental imagery—was related to better memory performance only in older age. The connectivity patterns supporting memory performance in older age reflected preservation of thickness of the medial temporal cortex. The results are more in accordance with a maintenance rather than a compensation account.

Key words: aging; functional connectivity; longitudinal MRI; memory encoding; psychophysiological interaction (PPI).

Introduction

Episodic memory declines with age (Rönnlund et al. 2005), although there is substantial interindividual variability in the trajectories (Nyberg et al. 2012). Variability in memory function is affected by changes in the structural and functional architecture of the brain. Hence, how brain regions communicate during memory tasks may be a key factor in explaining age-related changes in memory performance as well as interindividual variation of performance in older age. Assessing brain functional connectivity changes in task contexts provides a window for studying age-related brain changes in response to specific cognitive demands (Campbell and Schacter 2017). In the present study, we used task-related functional magnetic resonance imaging (fMRI) in a large adult lifespan sample to address 3 questions: (1) is higher age associated with differences in task-connectivity during encoding? Specifically, from previous literature we expected decreased intranetwork connectivity within the default-mode network (DMN) and increased internetwork connectivity between

regions involved in higher cognitive functions such as between the control and dorsal attention networks. Such patterns have been seen both in whole-brain resting-state (Geerligs et al. 2015) and region-of-interest (ROI)-based task-connectivity studies (Grady et al. 2016; Spreng et al. 2016). (2) Do encoding connectivity patterns associated with memory encoding overlap with the activity signatures of specific cognitive processes? If so, this will inform about additional cognitive processes associated with encoding. (3) Is connectivity associated with memory encoding performance related to longitudinal brain structural and cognitive changes as measured over eight years? This addresses the question of the importance of brain maintenance for cognitive function (Nyberg et al. 2012).

Cognitive processes arise from large-scale synchronization of neural interactions among areas across the brain. These areas are not necessarily restricted to a priori selected regions that can be detected in activity-based contrasts (Stanley et al. 2019). So far, few studies have addressed whole-brain fMRI connectivity during

memory encoding (Wang et al. 2010; Matthäus et al. 2012; Grady et al. 2016). Rather, most previous studies on functional connectivity changes in aging have employed seed-based task-functional connectivity (Grady et al. 2003; Oh and Jagust 2013), or resting-state fMRI (rs-fMRI) (Fjell et al. 2015). Seed-based task-connectivity studies have repeatedly found higher age to be related to stronger positive connectivity between medial temporal lobe (MTL), most notably the hippocampus, and prefrontal areas (PFC), during encoding of scenes and words (Grady et al. 2003; Oh and Jagust 2013). Research using rs-fMRI has found decreased positive intranetwork connectivity with higher age—especially within the default-mode regions—and increased connectivity between networks such as the dorsal attention and the DMN (Vidal-Piñeiro et al. 2014; Sala-Llonch et al. 2015). However, encoding connectivity exhibits a substantially different pattern from that observed during rest (Keerativittayayut et al. 2018). Therefore, it is crucial to understand how whole-brain task-connectivity during memory encoding contributes to successful recollection.

Encoding-based connectivity during an incidental encoding-task has been characterized by increased communication between distant areas, such as higher integration of default mode, salience, and subcortical networks with the other subnetworks (Keerativittayayut et al. 2018). Furthermore, flexible nodes—nodes that change network membership during different episodic memory task phases—appear to be relevant for memory performance as degree of observed reorganization between states partially predicts retrieval success (Schedlbauer and Ekstrom 2019). The small number of studies that have tested age-related differences in whole-brain connectivity, during memory encoding (Wang et al. 2010; Matthäus et al. 2012; Grady et al. 2016) used a graph-theory framework to a combined set of different fMRI tasks (encoding of pictures and words presented). Wang et al. (2010) combined encoding and retrieval runs and found higher age to be associated with lower long- and short-range functional connections of frontal regions and higher regional centrality of posterior parietal areas. Matthäus et al. 2012 followed a similar approach and observed age-related increases in the density and size of the networks together with reduced efficiency of information processing during encoding. Finally, King et al. (2018) used a similar approach to the present one in a study of recollection memory. They ran a whole-brain psychophysiological interaction (PPI) analysis to examine age-differences, and found lower positive connectivity changes in older than young participants in visual, parietal, cingulate and dorsolateral regions during the recollection phase of a memory task.

Age-related functional changes may accompany brain structure decline. Maintenance, compensation, and reserve are complementary concepts, which may explain age-related differences in brain structural and functional characteristics. For instance, in one face-name paired

fMRI task, in accordance with the brain maintenance framework (Nyberg et al. 2012), older adults showing longitudinally positive increases in prefrontal activity—and in further areas beyond task-specific regions—exhibited greater memory and hippocampal volume decline (Persson et al. 2006; Pudas et al. 2018). Maintenance posits that, in older participants, relative structural integrity over time or patterns of connectivity similar to those observed in younger adults are associated with positive cognitive performance. Alternatively, age-differences in connectivity may reflect an attempt to compensate for neural breakdown (Cabeza et al. 2018). For instance, one scene pictures task-fMRI study found that positive connectivity between PFC with brain regions such as the visual, parietal, operculum cortices, and subcortical structures was related to better memory performance uniquely in older adults (Deng et al. 2021). This was interpreted in accordance with a compensatory account for the age-related connectivity changes, accompanied by MTL connectivity reconfiguration deficit. Evidence for compensation requires for successful memory performance in older adults, deployment of additional neural resources, or engagement of different brain areas compared to young participants. The concept of reserve refers to the phenomenon that there is no simple relationship between brain lesions and cognitive decline, and this discrepancy is assumed to reflect people various degrees of resilience or "reserve" (Stern et al. 2020). In addition, coupling age-related differences in function with cross-sectional performance is however not without problems, as compensatory responses can lay anywhere along a continuum from (partial) failure to success (Grady 2012). Hence, for a better and complete understanding, functional differences need to be associated with brain and cognitive changes assessed over time. This allow us to disentangle whether differences in brain function relate to age-related brain changes or rather reflect lifelong variations (brain reserve) (Cabeza et al. 2018; Stern et al. 2020).

Here we investigated age-related differences in functional connectivity during an associative encoding task using a whole-brain correlational PPI (cPPI) approach (Fornito et al. 2012) in a sample encompassing the entire adult age range ($n = 488$). We assessed connectivity changes during encoding associated with age, memory performance, and the interaction between age and memory.

Moreover, by comparing connectivity maps with meta-analytic activity maps, we investigated whether encoding connectivity patterns overlapped with the activity signatures of specific cognitive processes. Finally, among older adults, we tested whether the connectivity changes associated with successful memory encoding were related to longitudinal structural and cognitive changes. This allowed us to test whether these functional patterns of connectivity should be interpreted in accordance with the maintenance or the compensation accounts.

Material and methods
Participants

A total of 488 participants (336 females, mean age = 41.65 years, SD = 17.20, age range = 18–81) were included in the final sample. All participants completed the fMRI tasks and were screened through health and neuropsychological assessments. Participants were required to have no history of neurological or psychiatric disorders, chronic illness, be right-handed, and not to use medicines known to affect nervous system functioning. Participants were further excluded based on the following neuropsychological criteria: score < 26 on the Mini-Mental State Examination (MMSE) (Folstein et al. 1975), score < 85 on the WASI II (Wechsler 1999), and a T-score of ≤ 30 on the California Verbal Learning Test II—Alternative Version (CVLT II) (Delis et al. 2000) immediate delay and long delay. All participants gave written informed consent, and the study was approved by the Regional Ethical Committee of South Norway and conducted in accordance with the Helsinki declaration. The concept of reserve a subsample of older participants (age > 50 years), spanning up to a maximum of 10 years back as follows: neuropsychological testing for 151 participants (n = 51, 6, and 94 with 1, 2, and ≥ 3 observations, respectively, 7.42 [1.94] years on average for those with at least 3 observations), and brain structural scans for 88 participants (n = 2, 5, and 81 with 1, 2, and ≥ 3 observations, respectively, 8.10 [0.93] years on average for those with at least 3 observations). Note that a small subsample of participants had retrospective data acquired with a different scanner. See Supplementary Table S1 for more information.

Experimental design and behavioral analysis

The experiment included an incidental encoding task and a memory test after approximately 90 min, both in the scanner. In this study, we only analyzed encoding fMRI data. The experimental design has been thoroughly described elsewhere (Sneve et al. 2015; Vidal-Piñeiro et al. 2019). See Figur 1 for a visual description of the experiment. In brief, the encoding and retrieval tasks consisted of 2 and 4 runs, respectively, that included 50 trials each. The stimulus material comprised 300 black and white line drawings of everyday items. A central fixation cross was shown during the baseline recording at the beginning, the middle, and the end of each run for 11 s. In the encoding phase, the trial started with a voice asking the participants either "Can you eat it?" or "Can you lift it?". Each question was asked 25 times in each run in a pseudorandomized order. One second after the question, an item appeared on the screen for 2 s, asking the participant to answer "Yes" or "No," before being replaced by a fixation cross that remained throughout the intertrial interval (between 1 and 7 s, exponential distribution; duration = 2.98 [2.49] s). In the retrieval phase, the trial started with Question 1: "Have you seen this item before?." The item appeared on the

screen for 2 s, and the participant had to press "Yes" (old item), or "No" (new item). In each run, 25 old items and 25 new items were presented in a pseudorandomized order. If the participant responded "No," the trial ended. If the participant responded "Yes," the trial proceeded to Question 2: "Can you remember what you were supposed to do with the item?." Again, if the participant responded "No," the trial ended, if "Yes" the trial continued with Question 3: "Were you supposed to eat it or lift it?." The participant was forced to choose between the 2 actions associated with the item at encoding. For behavioral analysis, the classification of responses to old items was: (1) source memory ("Yes" response to Question 1 and Question 2, and correct answer to Question 3), (2) item memory ("Yes" response to Question 1 and either "No" to Question 2 or incorrect answer to Question 3), (3) miss (incorrect answer to Question 1). New items were classified either as (4) correct rejections or (5) false alarms. Memory performance in the task was calculated as the proportion of source memory minus incorrect judgments to Question 3 (wrong recollection), tentatively controlling for false memories and guessing behavior (Vidal-Piñeiro et al. 2019). This measure is useful for capturing the associative features of memory encoding performance which are strongly affected by age (compared to recognition-based indices) (Old and Naveh-Benjamin 2008). The relationship between age and relevant behavioral and neuropsychological metrics was tested with generalized additive models (GAMs), controlling for sex.

MRI acquisition

Imaging data were collected using a 20-channel Siemens head–neck coil on a 3 T MRI (Siemens Skyra Scanner, Siemens Medical Solutions, Germany) at Rikshospitalet, Oslo University Hospital. The functional imaging parameters were equivalent across all fMRI runs: 43 transversally oriented slices (no gap) were measured using a BOLD-sensitive T2*-weighted EPI sequence (TR = 2390 ms, TE = 30 ms, flip angle = 90°, voxel size = 3 × 3 × 3 mm³, FOV = 224 × 224 mm², interleaved acquisition; generalized autocalibrating partially parallel acquisitions acceleration factor [GRAPPA] = 2). Each encoding run produced 134 volumes. At the start of each fMRI run, 3 dummy volumes were collected to avoid T1 saturation effects. Anatomical T1-weighted (T1w) magnetization-prepared rapid gradient echo (MPRAGE) images consisting of 176 sagittally oriented slices were obtained using a turbo field echo pulse sequence (TR = 2300 ms, TE = 2.98 ms, TI = 850 ms, flip angle = 8°, voxel size = 1 × 1 × 1 mm³, FOV = 256 × 256 mm²) were also acquired. Furthermore, a standard double-echo gradient-echo field map sequence was acquired for distortion correction of the echo planar images. Visual stimuli were presented in the scanner environment with an NNL 32-inch LCD monitor while participants responded using the ResponseGrip device (both Nordic-NeuroLab, Norway). Auditory stimuli were presented to
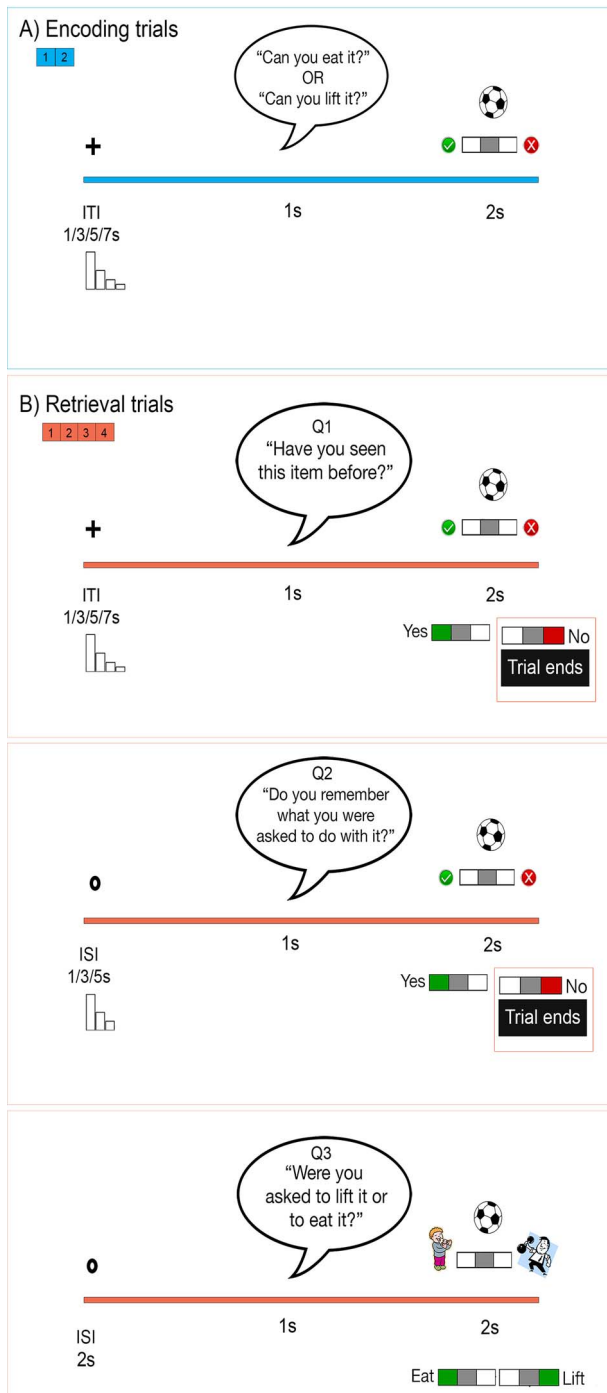
Fig. 1. Experimental paradigm. (A) 1 trial of the encoding task. The green checkmark and the red X were present on the screen to indicate which button indicate yes and no. (B) 1 trial of the retrieval task. Test questions 1 and 2 required a yes/no response, whereas question 3 required a choice between the two actions. The trial ended if the participant responded no to either 1 of the 2 first questions. Response cues (checkmark, X, eating, lifting) were also present on the screen. ITI intertrial interval, ISI interstimulus interval. Adapted from Vidal-Piñeiro et al. (2017).

the participants' headphones through the scanner intercom. The structural T1w data used in the longitudinal analysis were collected using a 12-channel head coil on a 1.5 T Siemens Avanto scanner (Siemens Medical Solutions, Germany) at Rikshospitalet, Oslo University Hospital. The pulse sequence acquired consisted of two repeated 160-slice sagittal T1-weighted MPRAGE sequences (TR = 2400 ms, TE = 3.61 ms, TI = 1000 ms, flip angle = 8°, voxel size = 1.25 × 1.25 × 1.20 mm, FOV = 240 mm). The raw images were automatically corrected for spatial distortion due to gradient nonlinearity (Jovicich et al. 2006) and field inhomogeneity (Sled et al. 1998), averaged, and resampled to isotropic 1 mm voxels.

MRI preprocessing
fMRI preprocessing

Data were organized and named according to the Brain Imaging Dataset Specification standard (*BIDS*) and pre-processed using a *fMRIPep* preprocessing pipeline (Esteban et al. 2019) (v. 1.2.5) a "Nipype" based tool (Gorgolewski et al. 2018) (v. 1.1.6).

The T1w image was corrected for intensity nonuniformity (INU) using *N4BiasFieldCorrection* (Tustison et al. 2010) (ANTs v. 2.2.0), and used as T1w-reference throughout the workflow. The T1w-reference was then skull-stripped using *antsBrainExtraction.sh* (ANTs v. 2.2.0), using OASIS as target template. Brain surfaces were reconstructed using recon-all (FreeSurfer v. 6.0.1) (Dale et al. 1999), and the brain mask estimated previously was refined with a custom variation of the method to reconcile ANTs-derived and FreeSurfer-derived segmentation of the cortical gray matter (GM) of *Mindboggle* (Klein et al. 2017). Spatial normalization to the ICBM152 Nonlinear Asymmetrical template version 2009c (Fonov et al. 2009) was performed through nonlinear registration with *antsRegistration* (Avants et al. 2008), using brain-extracted versions of both T1w volume and template. Brain tissue segmentation of cerebrospinal fluid, white-matter and gray matter was performed on the brain-extracted T1w using FAST (FSL v. 5.0.9) (Zhang et al. 2001).

For each BOLD run, the following preprocessing was performed: first, a reference volume and its skull-stripped version were generated using a custom methodology of fMRIPrep. A deformation field to correct for susceptibility distortions was estimated based on a field map that was coregistered to the BOLD reference, using a custom workflow of fMRIPrep derived from D. Greve's *epidewarp.fsl* script and further improvements of HCP Pipelines (Glasser et al. 2013). Dummy scans, acquired at the beginning of each BOLD run, were averaged and used as reference due to their superior tissue contrast. Based on the estimated susceptibility distortion, an unwarped BOLD reference was calculated for a more accurate coregistration with the anatomical reference. The BOLD reference was then co-registered to the T1w reference using *bbregister* (FreeSurfer). Coregistration was configured with 6 degrees of freedom. Head-motion parameters with respect to the BOLD reference (transformation matrices, and 6 corresponding rotation and translation parameters) were estimated before any spatiotemporal filtering using *mcflirt* (FSL v. 5.0.9) (Jenkinson et al. 2002). BOLD runs were slice-time corrected using *3dTshift from AFNI v. 20,160,207* (Cox and Hyde 1997). The BOLD time-series (including

slice-timing correction when applied) were resampled onto their original, native space by applying a single, composite transform to correct for head-motion and susceptibility distortions. These resampled BOLD time-series will be referred to as preprocessed BOLD in original space, or just preprocessed BOLD. Several confounding time-series were calculated based on the preprocessed BOLD: framewise displacement (FD) was calculated for each functional run, using Nipype's implementation (following the definitions by Power et al. (2014)). Additionally, a set of physiological regressors were extracted to allow for component-based noise correction (*CompCor*) (Behzadi et al. 2007). Principal components were estimated after high-pass filtering the preprocessed BOLD time-series (using a discrete cosine filter with 128 s cut-off). A subcortical mask was obtained by heavily eroding the brain mask to ensure it would not include cortical gray matter regions. Six anatomical CompCor (aCompCor) components were then calculated within the intersection of the aforementioned mask and the union of cerebrospinal fluid and white matter masks calculated in T1w space, after their projection to the native space of each functional run (using the inverse BOLD-to-T1w transformation). Preprocessed BOLD data were denoised prior to statistical analyses via the FSL-function fsl_regfilt (FSL v. 5.0.10). This involved regressing out the 6 aCompCor (Behzadi et al. 2007) components together with head-motion estimates (3 translation + 3 rotation parameters). All resamplings were performed with a single interpolation step by composing all the pertinent transformations (i.e. head-motion transform matrices, susceptibility distortion correction when available, and coregistrations to anatomical and template spaces). Gridded (volumetric) resamplings were performed using *antsApplyTransforms* (ANTs), configured with Lanczos interpolation to minimize the smoothing effects of other kernels (Lanczos 1964). Nongridded (surface) resamplings were performed using *mri_vol2surf* (FreeSurfer).

Correlational PPI estimation

We estimated the first-level whole-brain PPI (cPPI) (Fornito et al. 2012) matrix in each subject's native space. Note that, in contrast with the traditional PPI technique, cPPI results in symmetrical, *undirected* connectivity matrices. We used a ROI-based approach, obtaining connectivity terms for $|N| = 416$ ROIs corresponding to the cortical Schaeffer parcellation ($|N| = 400$) (Schaefer et al. 2018) and 8 bilateral ROIs from the *aseg* atlas (accumbens, amygdala, caudate, pallidum, putamen, thalamus, hippocampus anterior, and posterior) (Fischl et al. 2002). Four "psychological" timeseries were set up as boxcar functions, reflecting 2 s encoding events that comprised the entire period of picture presentation. Events were assigned to a given condition based on the participant's response during the subsequent memory test namely: Source (subsequent item-source association [Yes response to Q1 and Q2 and correct response to Q3]), Item (subsequent item memory without memory for the

association [correct Yes response to Q1 and either a No response to Q2, or incorrect response to Q3]), Miss memory trials, and trials with no response. Next, denoised BOLD timeseries from the 416 ROIs were deconvolved into neuronal estimates (Gitelman et al. 2003) and point-by-point multiplied with the psychological event time-series. The resulting "psychophysiological" timeseries, one per event type, were returned to the BOLD level through convolution with a canonical 2-gamma HRF, becoming our PPI-terms. cPPI matrices were established for each participant and task event type separately via partial Pearson's correlations, correlating BOLD-level PPI terms extracted from pairs of ROIs while controlling for (i) PPI-terms representing other task events, (ii) both ROIs' denoised BOLD timeseries, (iii) HRF-convolved versions of the psychological timeseries. The resulting partial correlation coefficients were Fisher-transformed to z values, and the full cPPI matrix for a given task event mean-centered within-individual before entering higher-level analysis. Note that cPPI values—when contrasted against the implicit baseline—capture both intrinsic connectivity and task-specific connectivity. This measure is thus more analogous to beta-series correlation and steady-state connectivity measures than to traditional PPI connectivity. Thus, our cPPI measures are affected—to some extent—by non-neural effects affecting intrinsic connectivity values; some of them associated with age. Demeaning effectively reduces the contribution of global undefined noise to participants' cPPI values, but also changes the values from absolute to relative measures of functional connectivity. As such, observed variability over participants reflect differences in nodes and edges' relative strengths in the graph, alternatively conceptualized as reflecting differences in prioritization within the functional connectome. For illustrative and communication purposes, the ROIs were grouped based on 18 networks (subcortical network plus 17 cortical networks as defined by Yeo et al. (2011)).

Longitudinal structural preprocessing

For the structural longitudinal analysis, we performed cortical reconstruction and volumetric segmentation of the T1w scans using the longitudinal FreeSurfer stream v.6.0 (Reuter et al. 2012) (http://surfer.nmr.mgh.harvard.edu/fswiki). The images were initially processed using the cross-sectional stream thoroughly described elsewhere (Dale et al. 1999; Fischl et al. 1999; Fischl and Dale 2000). The automated processing pipeline includes removal of nonbrain tissues, Talairach transformation, intensity correction, tissue and volumetric segmentation, cortical surface reconstruction, and cortical parcellation. Next, an unbiased within-subject template volume based on all cross-sectional images was created for each participant, using robust, inverse consistent registration (Reuter et al. 2010). The processing of each time point was then reinitialized with common information from the within-subject template, significantly increasing reliability and statistical power. Before group analysis, cortical

hemispheres were brought to *fsaverage* space and surface smoothing was applied at 12 mm FWHM. For subcortical structures (i.e. hippocampi) mean bilateral volume for specific structures was used in the analyses.

Higher-level analysis

Main effects of whole-brain correlational PPI

We ran four GLM models on the whole-brain connectivity cPPI matrices to assess the mean connectivity and the effects of age, performance, and age × performance interaction. Sex was used as a covariate of no-interest in all models. The models were built in a step-wise manner, adding complexity in each model. First, we assessed the mean patterns of task-dependent connectivity during source memory encoding. Next, we added an age regressor to test for changes in encoding-connectivity with age. The third model tested the relation of performance (as defined by the corrected source memory scores) on encoding connectivity, age controlled. In the fourth model, we tested the age × performance interaction by adding the interaction regressor. This later model was restricted to edges showing a main effect of performance. The covariates were mean-centered. All analyses were corrected for multiple comparisons via cluster correction routines from the Network Based Statistics (NBS) toolbox (Zalesky et al. 2010), with $P < 0.01$ cluster-forming threshold and $P < 0.025$ (2 comparisons) cluster significance as determined by permutation testing ($n = 5000$).

Spatial relationship between connectivity maps and term-based meta-analyses

To further test the resulting connectivity patterns in relation to the specific cognitive processes involved, we investigated whether these encoding patterns overlapped with existing patterns of fMRI activity previously described in the literature. Hence, we compared the topology of the main effects of age, performance, and age × performance interaction with the meta-analytic patterns of activity that were associated with specific cognitive processes.

For connectivity, we estimated the "significance degree" of each ROI in the cPPI graphs; that is the number of connections ("edges") that were significant for a given ROI in a given contrast (age, performance, and age × performance interaction). The connectivity output for each contrast was a $|N| = 416$ ROIs map representing the degree to which each region was related to age, performance, and age × performance interaction effects.

The meta-analytic cognitive maps were computed with the *NiMARE* package (Salo et al. 2018), which uses core functions from *Neurosynth* (Yarkoni et al. 2011). The software computes meta-analytical maps based on (mostly) activity contrasts in fMRI studies using automated text mining and coordinate extraction tools. We restricted the meta-analytical terms to those that overlapped between the Neurosynth database and the cognitive atlas (Poldrack et al. 2011) ($|N| = 123$ terms) thus restricting terms to specific "mental processes"

(cognitive and emotional). Coordinate-based multilevel kernel density analysis (MKDA) models were used to model the specificity of the cognitive processes on neuroimaging data (Wager et al. 2009). Specificity refers to the probability of a cognitive term occurring given activation in a specific brain area. We set a term frequency threshold = 0.001 and a kernel radius = 10 mm. The remaining parameters were left to default. For comparison with "significance degree" from connectivity, the resulting meta-analytical maps were parcellated into $|N| = 416$ ROIs using a volumetric parcellation.

The relationship between the "significant degree" and the meta-analytical cognitive maps was assessed using Pearson's correlations. Permutation-based significance testing ($P \leq 0.01$) was performed with the *BrainSMASH* package (Brain Surrogate Maps with Autocorrelated Spatial Heterogeneity) (Burt et al. 2020). *BrainSMASH* enables statistical testing of spatially correlated brain maps by simulating surrogate brain maps with a spatial autocorrelation that matches the target map; here the meta-analytical cognitive maps (Viladomat et al. 2014). Surrogate maps ($n = 5000$) were generated based on a Euclidean distance matrix of the center-of-gravity ROI coordinates. A null distribution was then defined by correlating the surrogate and the "significant degree" maps.

Relationship between connectivity patterns in older age and brain structural decline

We studied the relationship between encoding connectivity and brain atrophy and cortical thinning in a subsample of older individuals with retrospective longitudinal data ($n = 81$, age > 50 years). The longitudinal data spanned back on average 8.1 (SD = 0.93) years; the timing of the last observation overlapped with the timing of the encoding task. We focused on the clusters that were associated with memory performance with increasing age. We used a summarized metric that consisted of mean encoding connectivity from the clusters identified in the age × performance interaction models (see above for more details). Hereafter, we refer to those metrics as *memory-positive* and *memory-negative in older age*, as the resulting clusters were associated either with higher and lower memory performance with higher age, respectively. We tested whether these patterns of connectivity were associated with whole-brain cortical thinning using spatiotemporal linear mixed effect (LME) modeling as implemented in Freesurfer (Bernal-Rusiel et al. 2013). LME models were run as a function of time (years from the experimental task), connectivity, and the connectivity × time interaction. Sex, estimated intracranial volume (eICV), and baseline age (last measurement) were introduced as covariates of no-interest and subject identifiers as random intercepts (Bernal-Rusiel et al. 2013). Statistical significance was tested at each cortical vertex and the resulting maps were corrected for multiple comparisons using false discovery rate (pFDR < 0.01). Finally, we investigated whether these patterns of connectivity were
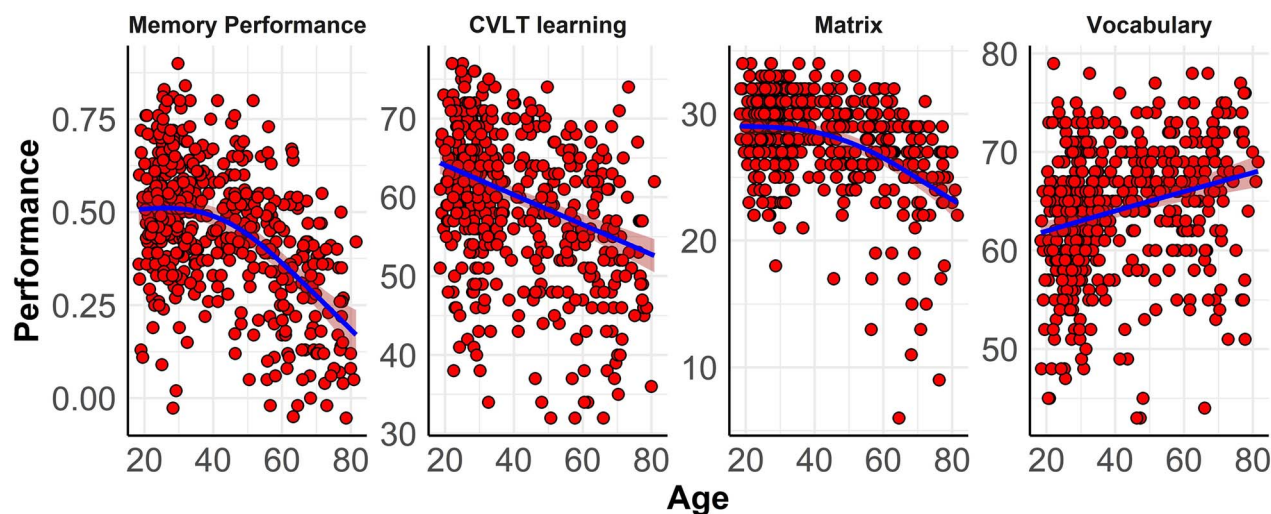
Fig. 2. Trajectories of cognition throughout the adult lifespan. Cognitive performance was fitted by age using GAMs, controlled for sex. Memory performance = corrected source memory score from the experimental task; CVLT learning = words learned and recalled across the five CVLT learning trials; vocabulary and matrix = WAIS-IV vocabulary and matrices reasoning raw scores. Ribbons represent 95% confidence intervals.

associated with decreased hippocampus volume, using the same model described above.

Relationship between connectivity patterns in older age and cognitive decline

We studied the relationship between encoding connectivity and decline in memory function and general cognition in a subsample of older individuals with retrospective longitudinal cognitive data. The longitudinal data spanned back on average 7.42 years (SD = 1.94); the last observation corresponded in time with the current experimental task. We selected total learning score from the California Verbal Learning Test (CVLT), and the Vocabulary and Matrix Reasoning test from the WASI-II battery as proxies for memory function, crystalized and fluid intelligence. To explore whether connectivity in the *memory-positive* and *memory-negative in older age* clusters were associated with cognitive decline over time we ran LME analyses as detailed above with the cognitive measures fitted as a function of time (years from the experimental task), connectivity, and the connectivity × time interaction (pFDR < 0.01). Sex and baseline age were introduced as covariates of no-interest and subject identifiers as random intercepts.

Results
Behavioral results

Memory performance in the fMRI task showed a nonlinear negative relationship to age, accelerating in the sixth decade of life ($F = 52.26$, edf = 2.60, [$P < 0.001$]) (edf informs about the degree of complexity of the gam response). The different cognitive measures were related to age (all P's < 0.001), controlling for sex; higher age was related to lower memory and visuospatial reasoning and higher vocabulary performance. See Figure 2 and Supplementary Table S2 for additional information.

Whole-brain encoding connectivity

In the main analyses, we assessed the effect of the mean task connectivity patterns during memory source memory encoding and their association with age, performance (corrected source memory score from the experimental task), and the age × performance interaction. See Supplementary materials in [Zenodo], at https://doi.org/10.5281/zenodo.5526077, for the significant edges for each main effect, and Supplementary Table S4 for the proportion of significant intranetwork and internetwork connections.

Mean encoding connectivity

Mean across-participants connectivity during encoding (Fig. 3A) was characterized by high intranetwork connectivity values and high internetwork connectivity between default-mode subnetworks and somatomotor networks. Low internetwork connectivity of salience, control, and limbic networks with subcortical, visual, somatomotor, and dorsal attention networks was seen.

Age effects

Pairwise connectivity between regions involved in higher cognitive functions and unimodal and attentional regions increased with higher age. Specifically, with age connectivity was higher between control, limbic, and default-mode subnetworks with somatomotor, visual, subcortical regions, and the dorsal attentional stream. Conversely, intranetwork connectivity within control, dorsal, a subnetwork of DMN and somatomotor networks was lower in older adults. See Figure 3B (positive relationship with age number of significant edges = 37,838; negative relationship with age number of significant edges = 38,022). Note negative age effects mean that the patterns were associated with younger age. As resulted from the Mantel test, we found an inverse relationship ($r = -0.19$, $P < 0.001$ from Mantel
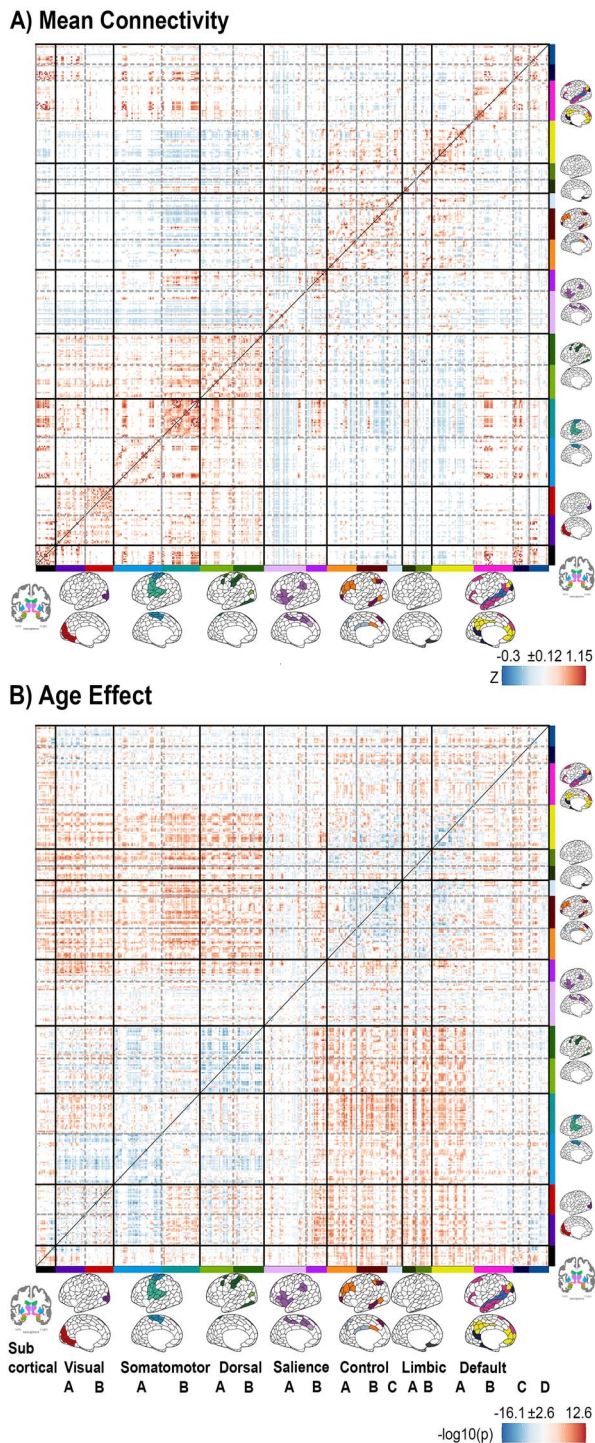
Fig. 3. P-values matrices for mean encoding connectivity and age effects. ROIs were grouped based on the Yeo-17 atlas (Yeo et al. 2011) and a subcortical network. Default D = TemporoParietal network. +/− values refer to the directionality of the findings, as contrasts employed are 2-tailed. Red represents higher connectivity values and positive age effects, while blue represents lower connectivity values and negative age effects. For the mean effect, only connections ≥1 SD of the mean are displayed. For the age effects, only connections in FWE-corrected significant clusters are displayed (P < 0.01). All the P-values have been transformed to −log10(P).

test [n = 10,000 permutations]) between the matrices of mean encoding connectivity and matrices of age effects, suggesting a likely "dedifferentiation" of the connectivity

patterns with higher age. The inclusion of performance in the model did not qualitatively affect the results.

Performance effects

Better memory performance (positive performance) in the task was associated with higher connectivity independently of age within posterior parietal and frontal regions, namely the superior parietal lobule, auditory and somatomotor areas, the frontal operculum and medial PFC regions (age, sex controlled; number of significant edges = 2,246; Fig. 4B). Conversely, poorer memory performance (negative performance) was associated with higher connectivity within posterior lateral DMN regions, medial DMN regions, dorsal PFC areas, lateral PFC areas, and the temporal pole (number of significant edges = 2838; Fig. 4C).

Age × performance interaction effects

Next, we tested whether there were age × performance interaction effects within the regions showing a main effect of performance. We found two significant (FWE controlled) clusters showing positive and negative age × performance interactions, respectively. See Figure 5 for a visual illustration. The first cluster *(memory-positive in older age)* included connectivity between medial temporal and posterior parietal regions, including the retrosplenial cortex, the inferior and superior parietal lobules, and regions in the MTL. Higher connectivity between these regions was associated with better performance with higher age (number of significant edges = 56 masked by 5,284 egdes; Fig. 5B). The second cluster *(memory-negative in older age)* corresponded to connections between frontal, parietal, and visual regions. Increased connectivity between these regions was associated with lower performance in older participants (number of significant edges = 42 masked by 5,284 egdes; Fig. 5C).

Spatial relationship between connectivity maps and term-based meta-analyses

Next, we tested the spatial relationship between the encoding connectivity patterns and the meta-analytic activity maps associated with specific cognitive processes (P ≤ 0.01 using a permutation-based approach). We used a "significance degree" *(number of significant connections for a given ROI in a given contrast)* and specificity metrics for connectivity patterns and cognitive maps, respectively. This was done for all connectivity effects of interest (age, performance, and age × performance interaction). See Figure 6 and Supplementary Table S3 for the full results. The connectivity patterns where greater connectivity was related to higher age (i.e. older age) overlapped significantly with the meta-analytic activity patterns of retrieval, recall, and encoding processes. Conversely, the connectivity patterns where greater connectivity was associated with lower age (i.e. younger age) overlapped with maps related to imagery, spatial attention, and movement activity. The connectivity patterns where greater connectivity was associated

A) Performance Effect
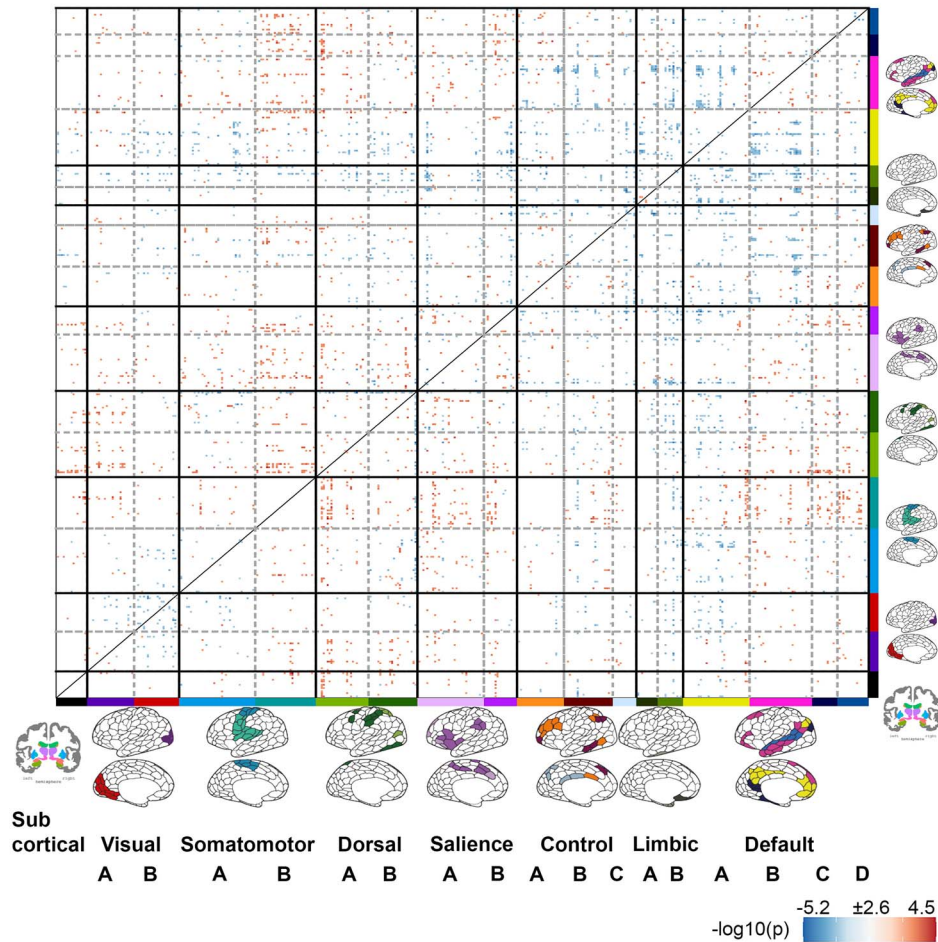
B) Positive Performance
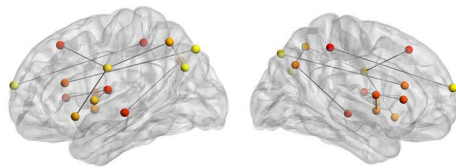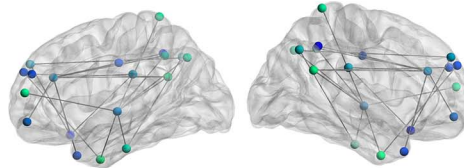
C) Negative Performance

Fig. 4. Performance effects. (A) *P*-values matrix for performance effects. Performance was defined as (corrected) source memory performance in the experimental task. ROIs were grouped based on the Yeo-17 atlas (Yeo et al. 2011) and a subcortical network. Default D = TemporoParietal network. +/− values refer to the directionality of the findings, as contrasts employed are 2-tailed. Red represents higher connectivity values and positive performance effects and vice versa for the blue scale. For the performance effects, only connections within FWE-corrected significant clusters are displayed (*P* < 0.01). All the *P*-values have been transformed to −log10(*P*). (B and C) Top 5% of significant nodes shown overlaid to 3D-brain BrainNet viewer (Xia et al. 2013 http://www.nitrc.org/projects/bnv/). Nodes are filled with red to yellow scales from lower to higher connections (and blue to turquoise from lower to higher connections) that indicate the number of connections ("significance degree"). Only edges between drawn nodes are displayed.

with better memory performance overlapped with multisensory, integration, and speech production areas. Connectivity patterns where greater connectivity was related to worse performance overlapped with maps associated with salience, emotion, and belief. The spatial patterns of connectivity associated with positive age × performance interaction (*memory-positive in older-age*) overlapped with the activity patterns associated with mental imagery. No terms were associated with negative age × performance interaction (*memory-negative in older*

age). These results inform us on cognitive processes that may be related to successful memory performance in successful aging, that is, integrative and multisensory strategies and mental imagery.
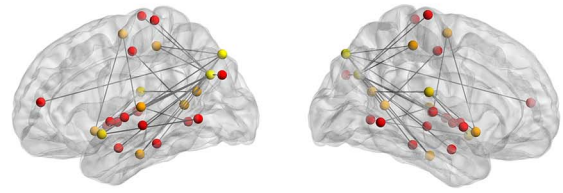
Relationship between connectivity patterns in older age and brain structural decline

We assessed the relationship between brain atrophy and cortical thinning and connectivity patterns in older age to investigate whether age-related connectivity changes

A) Slope Age×Performance Effect
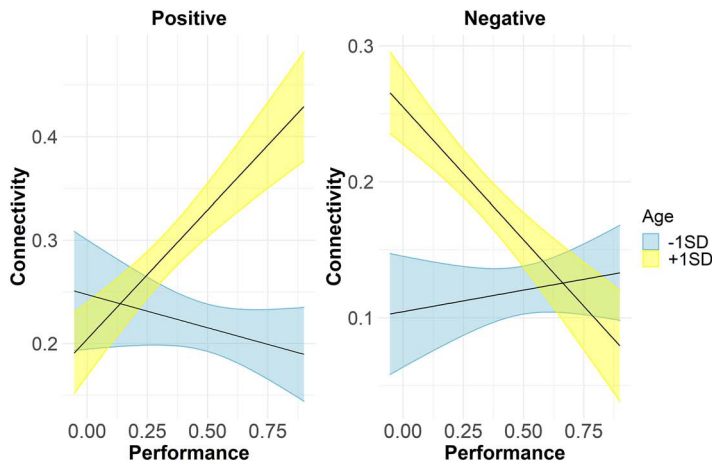
B) Memory-positive in older age

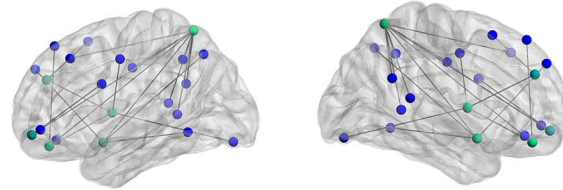**C) Memory-negative in older age**

Fig. 5. Age × performance interaction effects. (A) Relationship between performance and task-dependent connectivity across age. For illustrative purpose, the effects of performance were predicted at two levels (± 1 SD age; mean age = 41.65 [SD = 17.18] years). Note though that age was introduced as a continuous regressor in the model. Ribbons represent 95% confidence intervals. (B and C) Top 5% of significant nodes shown overlaid to 3D-brain BrainNet viewer (Xia et al. 2013 http://www.nitrc.org/projects/bnv/). Nodes are filled with red to yellow scales from lower to higher connections (and blue to turquoise from lower to higher connections) that indicate the number of connections ("significance degree"). Only edges between drawn nodes are displayed.
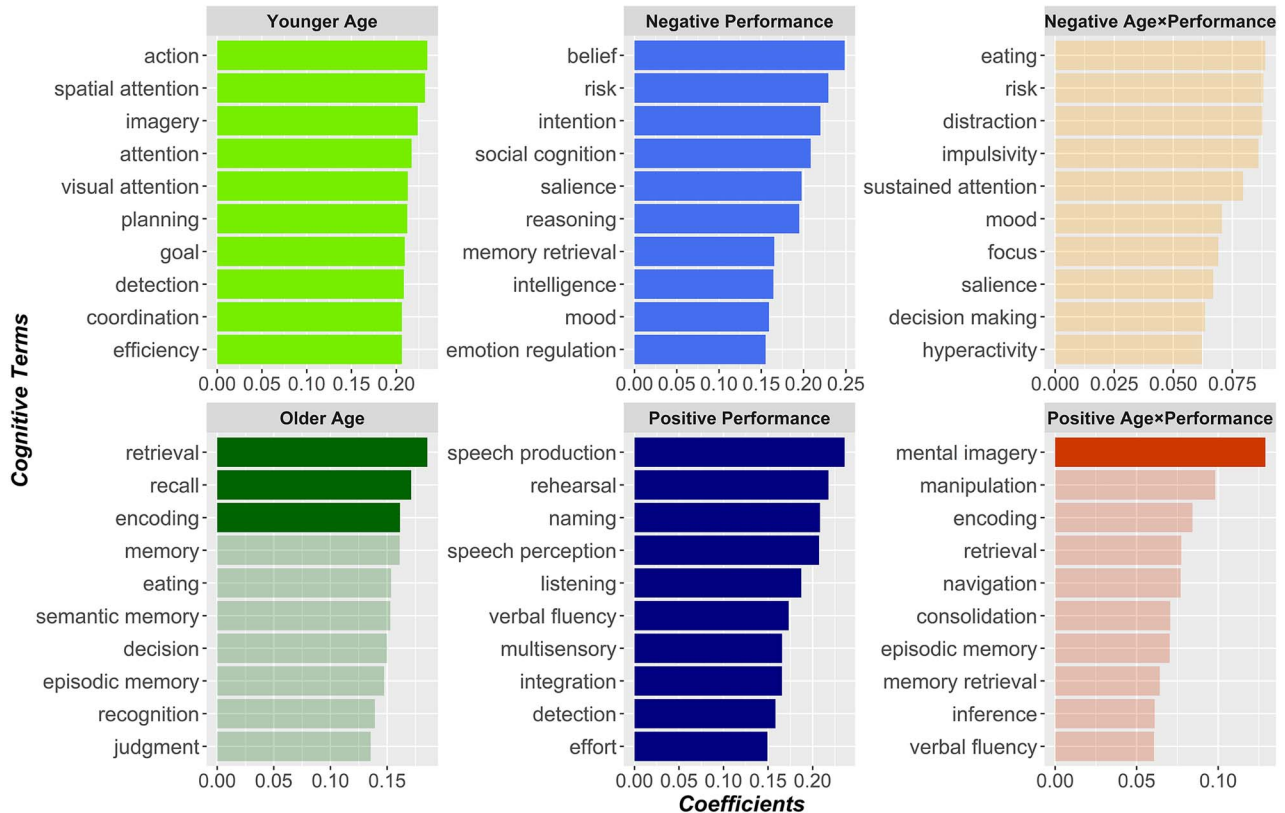

Fig. 6. Spatial relationship between connectivity maps and meta-analytic patterns associated with specific cognitive processes. We displayed the top cognitive terms associated with each contrast. Opaque colors reflects terms that survived the significance threshold ($P \leq 0.01$) as determined by a permutation approach using BrainSMASH (Burt et al. 2020). X-axis represents the empirical Pearson's correlation (r), note that different ranges are depicted for each contrast.

reflected maintenance or compensatory responses. This analysis was performed in a subsample of older participants ($n = 81$, age > 50) with retrospective longitudinal neuroimaging data (see Supplementary Table S1). A linear mixed effects analysis (controlled for sex, eICV, and baseline age) revealed that the cluster related to

Memory patterns of connectivity in older age and brain structural decline over time
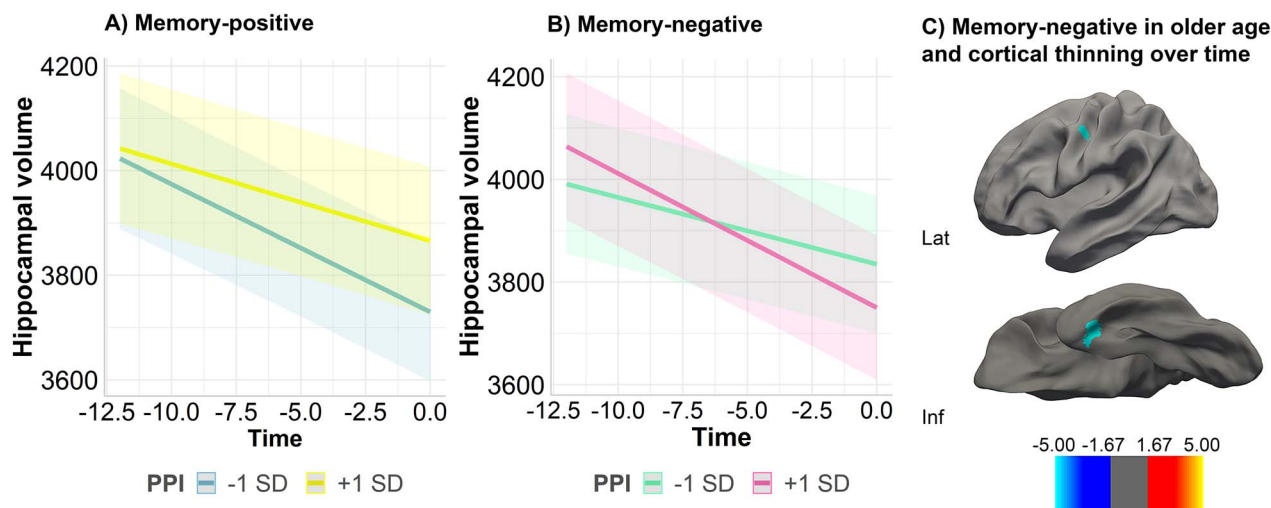

Fig. 7. Relationship between memory pattern of connectivity in older age and decline of brain structures over time. (A and B) Relationship between memory patterns of connectivity in older and longitudinal structural hippocampal volume. (A) The yellow line represents higher memory performance in memory-positive cluster. (B) The pink line represents lower memory performance in memory-negative cluster. Results are significant at pFDR < 0.01. Values were predicted at eICV, and baseline age. (C) Whole-brain cortical thickness decline is associated with the memory-negative connectivity cluster in older age. Only regions showing significant thinning over time are shown. Left hemisphere. Maps are corrected for multiple comparisons at pFDR < 0.01. In the colorbar –log10(P) values are displayed, red/yellow represents higher values, blue/cyan lower values.

higher memory performance in older age *(memory-positive in older age)* was associated with less hippocampal volume decrease over time ($F = 44.2$, df = 165, $P < 0.001$; Fig. 7A). In contrast, the cluster associated with lower memory performance in older age (memory-negative in older age) was related to a steeper volumetric decline of hippocampi ($F = -65.71$, df = 165, $P < 0.001$; Fig. 7B) and cortical thickness decline over time. Indeed, the cortical analysis showed a positive association between connectivity in this *memory-negative in older age* cluster and cortical thinning in two small clusters encompassing (1) the left precentral and (2) the anterior fusiform and the entorhinal cortices (pFDR < 0.01, Fig. 7C). The relationship between the connectivity cluster associated with the memory-positive connectivity cluster in older age and whole-brain cortical thinning did not survive multiple comparison corrections. Cortical thickness data are available longitudinally and retrospectively, but the association between cortical thinning and functional connectivity is better understood as an association rather than a causal prediction. Overall, the results supported the hypothesis that the patterns of connectivity associated with higher and lower performance in older age were related to structural maintenance versus decline of brain regions involved in memory processes.

Relationship between connectivity patterns in older age and cognitive decline

We assessed the relationship between memory patterns of connectivity in older age and cognitive decline using retrospective cognitive data (age > 50). See Supplementary Table S1 for details. LME models (controlled for sex and baseline age) revealed a relationship between

connectivity patterns associated with higher memory performance in older age *(memory-positive in older age)* and less decline in CVLT learning scores. However, the association did not survive multiple comparison corrections (pFDR = 0.07).

Discussion

We estimated whole-brain functional connectivity during episodic memory encoding, specifically focusing on age-related differences in connectivity and how they were associated with memory performance across the lifespan. In higher age, we found lower intranetwork and higher internetwork connectivity between regions involved in higher cognitive functions and the dorsal attention stream, sensorimotor and subcortical regions during encoding. Successful memory performance in higher age overlapped with networks involved in mental imagery. Among older adults, greater hippocampal and cortical atrophy was related to less favorable connectivity changes, reflecting maintenance processes over time.

The age effects on encoding connectivity are partially in agreement with previous rs-fMRI and task-fMRI studies, suggesting that some of the functional age-differences are task-independent. For example, several resting-state fMRI studies have found lower positive intranetwork connectivity and higher positive internetwork connectivity, suggesting that brain networks become less specialized during aging and the flow of information transmitted becomes less efficient (Betzel et al. 2014; Geerligs et al. 2015; Sala-Llonch et al. 2015). In our case, lower intranetwork connectivity

was found among networks supporting higher level cognitive functions, such as control, dorsal, and a subnetwork of DMN (comprising inferior parietal lobule, dorsal PFC and medial PFC). A similar pattern was found within somatomotor areas. In line with a rs-fMRI study of Geerligs et al. (2015), we found both increased internetwork connectivity between visual and control networks and reduced connectivity between visual and somatomotor networks during the task. Given the integration of the different types of stimuli required by the encoding task and the loss of intranetwork communication within high processing networks typically seen in aging, the increased connectivity of these networks with unimodal regions may reflect the need for older adults to cope with the higher demands of the encoding task. Moreover, we found higher age-related connectivity between control and dorsal attention networks, which has been reported previously in a fMRI study using a different task (Grady et al. 2016). This might be interpreted as an over-recruitment of cognitive control processes due to the cognitive demands of the task. Likewise, higher connectivity between inversely engaged networks, such as the control and the dorsal attention respectively with the default-mode, has been described in several tasks in aging (Spreng et al. 2016; Spreng and Turner 2019). These patterns may reflect age-related features during memory tasks such as lower flexibility in shifting from external and internal attention and semantization of cognition as older individuals might rely more on acquired knowledge. Although speculative, this interpretation receives further support from our results as the connectivity patterns associated with older age mapped unto cognitive processes such as retrieval and recall, suggesting that older participants might rely more on already acquired knowledge and schematic information during the encoding task. However, our results also reveal task-specific changes in connectivity. Compared to fMRI acquired during resting-state and other cognitive domains, we also identified the spatial correspondence between the connectivity patterns and cognitive maps, informing us on the specific cognitive processes possibly involved in the task. Younger people exhibited higher connectivity between areas overlapping with regions known to support cognitive processes relevant for our encoding task such as visual attention, action, and imagery. Some of these strategies may also have been adopted by older participants that performed better, which may be interpreted to be in accordance with the maintenance process framework. Taken together, the whole-brain approach and the analysis assessing the spatial overlap with established cognitive functions provides contributes to our understanding of task-related connectivity differences in aging above and beyond specific fMRI studies.

We found that the relationship between connectivity and memory performance differed as a function of age. Older people who performed better showed higher connectivity between medial temporal and posterior parietal

regions, including the retrosplenial cortex. As shown in a previous rs-fMRI study of older participants (Kaboodvand et al. 2018), episodic memory performance was positively associated with functional connectivity between the retrosplenial cortex and the MTL. The retrosplenial cortex is a key mediator in facilitating the communication between medial temporal and other DMNs regions, leading to memory performance success (Kaboodvand et al. 2018). In our study, the connectivity changes that were related to better performance in older participants overlapped spatially with the maps associated with mental imagery, in which the engagement of the retrosplenial cortex is widely described (Chrastil 2018). These strategies and functional connectivity changes mimicked those associated with younger age.

We found that the patterns of connectivity associated with successful performance in older participants were related to longitudinal volumetric maintenance of the hippocampus, critically involved in memory encoding. This is in agreement with the maintenance theory of cognitive aging (Nyberg et al. 2012), as hippocampal decline is a main factor behind memory decline in older age (Gorbach et al. 2017). Note that longitudinal studies allow us to distinguish between *aging* effects and lifelong constant differences, and thus are highly relevant to interpret cross-sectional changes in fMRI activity. Conversely, we found no evidence that the pattern of connectivity associated with higher performance in older age reflected a compensatory attempt to overcome structural decline. The widespread over-recruitment of different regions in frontal, parietal, and visual areas was not related to memory performance. Indeed, these connectivity changes were associated with lower performance and structural loss in the MTL over time, regions that typically show steep annual thickness decline in normal aging (Fjell and Walhovd 2010). Cognitive decline was associated with structural decline and a maladaptive organization in the functional architecture, whereas successful memory performance in older participants reflected relative structural integrity over time and functional connectivity changes that supported the use of "younger" cognitive strategies such as mental imagery. The results fit the maintenance framework more than the compensation framework. The study could have been contextualized using the reserve framework (Stern et al. 2020). Yet, since (cognitive) reserve traditionally focuses on proxies (IQ, education, bilingualism, mental leisure activities), we think compensation is a more relevant concept in this study. Indeed, our main goal was to understand, given the challenges of this specific task, whether individual differences in successful memory performance reflected the use of preserved or additional patterns of connectivity, rather than being explained in terms of different levels of a specific reserve proxy. Older participants who exhibited maintenance of connectivity patterns supporting memory function and strategies similar to those observed in younger adults, showed better memory performance. Between-person differences in

the rates of brain decline may be partially explained by cumulative environmental and biological effects over time (reserve) and before age-related changes. Indeed, these factors may have been translated into improved neural resources accumulated over time and able to counteract brain decline until some threshold, along with ongoing repair mechanisms able to preserve neural resources. However, we did not assess the single contribution of these factors, e.g. education, physical exercise, genetic variables, on building up maintenance and reserve mechanisms.

Limitations and methodological remarks

fMRI during task performance is suited for investigating brain dynamics underlying specific cognitive processes. Participants performing a task during scanning yield a degree of experimental control compared to resting-state (Campbell and Schacter 2017). cPPI captures both intrinsic and task-specific patterns of connectivity (akin to a steady-state sequence; see below). Despite commonalities across states, the functional brain architecture differs across the different task contexts (Davis et al. 2017). Brain regions reconfigure their connectivity patterns in a flexible way based on the current demands of the task (Cole et al. 2013). In the present study, the connectivity patterns associated with successful memory performance mapped on networks involved in cognitive processes relevant for the task. This provides information about brain organization changes associated with specific cognitive process of interest. However, *for this reason, a main disadvantage of task-fMRI is that differences* in the experimental design may hamper generalization (Damoiseaux and Huijbers 2017) across studies. In this study, some of our findings agree with previous rs-fMRI and task-fMRI research and thus likely represent task-invariant features of the aging brain (e.g. less specialized brain networks and lower flexibility in shifting from external to internal attention). However, other findings, *such* as the spatial correlation between functional connectivity and mental imagery processes, seem more constrained to the specific demands of the task and may only be replicable in paradigms where certain cognitive processes are beneficial for task performance.

The cPPI framework allowed for a whole-brain *undirected* (symmetric) assessment of task connectivity. cPPI does not imply inferences of directionality. The cPPI connectivity values reflect correlations between regions during selected task-periods of an fMRI run, controlling for stimulus-driven cofluctuations and intrinsic functional connectivity between the ROIs. When cPPI connectivity values estimated from different task-periods are subtracted, the resulting metric is largely comparable to traditional regression-based PPI approaches. However, when conditions are not subtracted—as in the current paper—cPPI is akin to "residualized" task-connectivity and beta series correlation, i.e. the similarity between two regions' trial-to-trial fluctuations in BOLD amplitude during task (Di et al. 2020). The different implications of the metrics

are largely omitted in the literature but have consequential implications for the interpretation, that is in this case, a task-state of integrated connectivity, instead of a shift in connectivity driven by the specific task.

The effects of demeaning data within participants are also consequential for the interpretation of our results. This approach minimizes the possibility of non-neural confounds that affect the implicit baseline being the main drivers of connectivity differences across individuals. Some of these confounds are known to be greatly correlated with age (Campbell and Schacter 2017). However, data demeaning only allowed us to interpret the results in relative terms, and in terms of reorganization. Note that many graph-theoretical studies use thresholded, binarized data and thus face a similar problem. It is however possible that some findings are a side-effect of this step. For example, the patterns of connectivity associated with lower performance in older participants are spatially unstructured and thus might represent unspecific changes in the functional connectome rather than reduced functional connectivity among specific regions.

Despite the structural and cognitive retrospective longitudinal data available, the main limitation of this study is the lack of longitudinal task-fMRI, which would have allowed us to assess how the functional architecture of the brain during memory tasks changes over time.

Conclusion

This study provides novel insights in whole-brain connectivity during encoding and its relation with age, cognitive processes, and structural decline in older age using a large sample encompassing the entire adulthood. Connectivity patterns underlying successful memory function in older age spatially mapped onto mental imagery processes and were related to structural brain maintenance over time. These results provide a bridge between the cognitive processes and the biological mechanisms that support memory function maintenance and decline in older age.

Supplementary material

Supplementary material is available at *Cerebral Cortex* online.

Funding

Conflict of interest statement. None declared.

References

Avants BB, Epstein CL, Grossman M, Gee JC. Symmetric diffeomorphic image registration with cross-correlation: evaluating automated labeling of elderly and neurodegenerative brain. *Med Image Anal*. 2008:12:26–41.

Behzadi Y, Restom K, Liau J, Liu TT. A component based noise correction method (CompCor) for BOLD and perfusion based fMRI. *NeuroImage*. 2007:37:90–101.

Bernal-Rusiel JL, Greve DN, Reuter M, Fischl B, Sabuncu MR. Statistical analysis of longitudinal neuroimage data with linear mixed effects models. *NeuroImage*. 2013:66:249–260.

Betzel RF, Byrge L, He Y, Goñi J, Zuo X-N, Sporns O. Changes in structural and functional connectivity among resting-state networks across the human lifespan. *NeuroImage*. 2014:102(Pt 2):345–357.

Burt JB, Helmer M, Shinn M, Anticevic A, Murray JD. Generative modeling of brain maps with spatial autocorrelation. *NeuroImage*. 2020:220:117038.

Cabeza R, Albert M, Belleville S, Craik FIM, Duarte A, Grady CL, Lindenberger U, Nyberg L, Park DC, Reuter-Lorenz PA, et al. Maintenance, reserve and compensation: the cognitive neuroscience of healthy ageing. *Nat Rev Neurosci*. 2018:19:701–710.

Campbell KL, Schacter DL. Ageing and the resting state: is cognition obsolete? *Lang Cogn Neurosci*. 2017:32:661–668.

Chrastil ER. Heterogeneity in human retrosplenial cortex: a review of function and connectivity. *Behav Neurosci*. 2018:132:317–338.

Cole MW, Reynolds JR, Power JD, Repovs G, Anticevic A, Braver TS. Multi-task connectivity reveals flexible hubs for adaptive task control. *Nat Neurosci*. 2013:16:1348–1355.

Cox RW, Hyde JS. Software tools for analysis and visualization of fMRI data. *NMR Biomed*. 1997:10:171–178.

Dale AM, Fischl B, Sereno MI. Cortical surface-based analysis. I. Segmentation and surface reconstruction. *NeuroImage*. 1999:9:179–194.

Damoiseaux JS, Huijbers W. The complementary value of task-evoked and resting-state functional imaging: a commentary on Campbell and Schacter (2016). *Lang Cogn Neurosci*. 2017:32:678–680.

Davis SW, Stanley ML, Moscovitch M, Cabeza R. Resting-state networks do not determine cognitive function networks: a commentary on Campbell and Schacter (2016). *Lang Cogn Neurosci*. 2017:32:669–673.

Delis DC, Kramer JH, Kaplan E, Ober BA. *Manual for the California verbal learning test (CVLT-II)*. San Antonio TX: Psychol Corp.; 2000

Deng L, Stanley ML, Monge ZA, Wing EA, Geib BR, Davis SW, Cabeza R. Age-related compensatory reconfiguration of PFC connections during episodic memory retrieval. *Cereb Cortex N Y N*. 2021:31(2):717–730.

Di X, Zhang Z, Biswal BB. Understanding psychophysiological interaction and its relations to beta series correlation. *Brain Imaging Behav*. 2020:15(2):958–973.

Esteban O, Markiewicz CJ, Blair RW, Moodie CA, Isik AI, Erramuzpe A, Kent JD, Goncalves M, DuPre E, Snyder M, et al. fMRIPrep: a robust preprocessing pipeline for functional MRI. *Nat Methods*. 2019:16:111–116.

Fischl B, Dale AM. Measuring the thickness of the human cerebral cortex from magnetic resonance images. *Proc Natl Acad Sci U S A*. 2000:97:11050–11055.

Fischl B, Sereno MI, Dale AM. Cortical surface-based analysis. II: inflation, flattening, and a surface-based coordinate system. *NeuroImage*. 1999:9:195–207.

Fischl B, Salat DH, Busa E, Albert M, Dieterich M, Haselgrove C, van der Kouwe A, Killiany R, Kennedy D, Klaveness S, et al. Whole brain segmentation. *Neuron*. 2002:33:341–355.

Fjell AM, Walhovd KB. Structural brain changes in aging: courses, causes and cognitive consequences. *Rev Neurosci*. 2010:21:187–221.

Fjell AM, Sneve MH, Grydeland H, Storsve AB, de Lange A-MG, Amlien IK, Røgeberg OJ, Walhovd KB. Functional connectivity change across multiple cortical networks relates to episodic memory changes in aging. *Neurobiol Aging*. 2015:36:3255–3268.

Folstein MF, Folstein SE, McHugh PR. "Mini-mental state". A practical method for grading the cognitive state of patients for the clinician. *J Psychiatr Res*. 1975:12:189–198.

Fonov V, Evans A, McKinstry R, Almli C, Collins D. Unbiased nonlinear average age-appropriate brain templates from birth to adulthood. *NeuroImage*. 2009:47:S102.

Fornito A, Harrison BJ, Zalesky A, Simons JS. Competitive and cooperative dynamics of large-scale brain functional networks supporting recollection. *Proc Natl Acad Sci*. 2012:109:12788–12793.

Geerligs L, Renken RJ, Saliasi E, Maurits NM, Lorist MM. A brain-wide study of age-related changes in functional connectivity. *Cereb Cortex*. 2015:25:1987–1999.

Gitelman DR, Penny WD, Ashburner J, Friston KJ. Modeling regional and psychophysiologic interactions in fMRI: the importance of hemodynamic deconvolution. *NeuroImage*. 2003:19:200–207.

Glasser MF, Sotiropoulos SN, Wilson JA, Coalson TS, Fischl B, Andersson JL, Xu J, Jbabdi S, Webster M, Polimeni JR, et al. The minimal preprocessing pipelines for the human connectome project. *NeuroImage*. 2013:80:105–124.

Gorbach T, Pudas S, Lundquist A, Orädd G, Josefsson M, Salami A, de Luna X, Nyberg L. Longitudinal association between hippocampus atrophy and episodic-memory decline. *Neurobiol Aging*. 2017:51:167–176.

Gorgolewski KJ, Esteban O, Markiewicz CJ, Ziegler E, Ellis DG, Jarecka D, Notter MP, Johnson H, Burns C, Manhães-Savio A, et al. Nipype 1.1.6. Software Zenodo. 2018. https://doi.org/10.5281/zenodo.1560596.

Grady C. The cognitive neuroscience of ageing. *Nat Rev Neurosci*. 2012:13:491–505.

Grady CL, McIntosh AR, Craik FIM. Age-related differences in the functional connectivity of the hippocampus during memory encoding. *Hippocampus*. 2003:13:572–586.

Grady C, Sarraf S, Saverino C, Campbell K. Age differences in the functional interactions among the default, frontoparietal control, and dorsal attention networks. *Neurobiol Aging*. 2016:41:159–172.

Jenkinson M, Bannister P, Brady M, Smith S. Improved optimization for the robust and accurate linear registration and motion correction of brain images. *NeuroImage*. 2002:17:825–841.

Jovicich J, Czanner S, Greve D, Haley E, van der Kouwe A, Gollub R, Kennedy D, Schmitt F, Brown G, Macfall J, et al. Reliability in multi-site structural MRI studies: effects of gradient nonlinearity correction on phantom and human data. *NeuroImage*. 2006:30:436–443.

Kaboodvand N, Bäckman L, Nyberg L, Salami A. The retrosplenial cortex: a memory gateway between the cortical default mode network and the medial temporal lobe. *Hum Brain Mapp*. 2018:39:2020–2034.

Keerativittayayut R, Aoki R, Sarabi MT, Jimura K, Nakahara K. Large-scale network integration in the human brain tracks temporal fluctuations in memory encoding performance. *elife*. 2018:7:e32696.

King DR, de Chastelaine M, Rugg MD. Recollection-related increases in functional connectivity across the healthy adult lifespan. *Neurobiol Aging*. 2018:62:1–19.

Klein A, Ghosh SS, Bao FS, Giard J, Häme Y, Stavsky E, Lee N, Rossa B, Reuter M, Chaibub Neto E, et al. Mindboggling morphometry of human brains. *PLoS Comput Biol*. 2017:13:e1005350.

Lanczos C. Evaluation of noisy data. *J Soc Ind Appl Math Ser B Numer Anal*. 1964:1:76–85.

Matthäus F, Schmidt J-P, Banerjee A, Schulze TG, Demirakca T, Diener C. Effects of age on the structure of functional connectivity networks during episodic and working memory demand. *Brain Connect*. 2012:2:113–124.

Nyberg L, Lövdén M, Riklund K, Lindenberger U, Bäckman L. Memory aging and brain maintenance. *Trends Cogn Sci*. 2012:16:292–305.

Oh H, Jagust WJ. Frontotemporal network connectivity during memory encoding is increased with aging and disrupted by Beta-amyloid. *J Neurosci*. 2013:33:18425–18437.

Old SR, Naveh-Benjamin M. Differential effects of age on item and associative measures of memory: a meta-analysis. *Psychol Aging*. 2008:23:104–118.

Persson J, Nyberg L, Lind J, Larsson A, Nilsson L-G, Ingvar M, Buckner RL. Structure–function correlates of cognitive decline in aging. *Cereb Cortex*. 2006:16:907–915.

Poldrack RA, Kittur A, Kalar D, Miller E, Seppa C, Gil Y, Parker DS, Sabb FW, Bilder RM. The cognitive atlas: toward a Knowledge Foundation for Cognitive Neuroscience. *Front Neuroinform*. 2011:5:17.

Power JD, Mitra A, Laumann TO, Snyder AZ, Schlaggar BL, Petersen SE. Methods to detect, characterize, and remove motion artifact in resting state fMRI. *NeuroImage*. 2014:84:320–341.

Pudas S, Josefsson M, Rieckmann A, Nyberg L. Longitudinal evidence for increased functional response in frontal cortex for older adults with hippocampal atrophy and memory decline. *Cereb Cortex*. 2018:28:936–948.

Reuter M, Rosas HD, Fischl B. Highly accurate inverse consistent registration: a robust approach. *NeuroImage*. 2010:53:1181–1196.

Reuter M, Schmansky NJ, Rosas HD, Fischl B. Within-subject template estimation for unbiased longitudinal image analysis. *NeuroImage*. 2012:61:1402–1418.

Rönnlund M, Nyberg L, Bäckman L, Nilsson L-G. Stability, growth, and decline in adult life span development of declarative memory: cross-sectional and longitudinal data from a population-based study. *Psychol Aging*. 2005:20:3–18.

Sala-Llonch R, Bartrés-Faz D, Junqué C. Reorganization of brain networks in aging: a review of functional connectivity studies. *Front Psychol*. 2015:6:663.

Salo T, Bottenhorn KL, Nichols TE, Riedel MC, Sutherland MT, Yarkoni T, Laird AR. NiMARE: a neuroimaging meta-analysis research environment. *F1000Research*. 2018:7:1221.

Schaefer A, Kong R, Gordon EM, Laumann TO, Zuo X-N, Holmes AJ, Eickhoff SB, Yeo BTT. Local-global parcellation of the human cerebral cortex from intrinsic functional connectivity MRI. *Cereb Cortex*. 2018:28:3095–3114.

Schedlbauer AM, Ekstrom AD. Flexible network community organization during the encoding and retrieval of spatiotemporal episodic memories. *Netw Neurosci*. 2019:3:1070–1093.

Sled JG, Zijdenbos AP, Evans AC. A nonparametric method for automatic correction of intensity nonuniformity in MRI data. *IEEE Trans Med Imaging*. 1998:17:87–97.

Sneve MH, Grydeland H, Nyberg L, Bowles B, Amlien IK, Langnes E, Walhovd KB, Fjell AM. Mechanisms underlying encoding of short-lived versus durable episodic memories. *J Neurosci*. 2015:35:5202–5212.

Spreng RN, Turner GR. The shifting architecture of cognition and brain function in older adulthood. *Perspect Psychol Sci J Assoc Psychol Sci*. 2019:14:523–542.

Spreng RN, Stevens WD, Viviano JD, Schacter DL. Attenuated anti-correlation between the default and dorsal attention networks with aging: evidence from task and rest. *Neurobiol Aging*. 2016:45:149–160.

Stanley ML, Geib BR, Davis SW. Chapter 10 - toward a more integrative cognitive neuroscience of episodic memory. In: Munsell BC, Wu G, Bonilha L, Laurienti PJ, editors. *Connectomics. The Elsevier and MICCAI society book series*. Academic Press; 2019. pp. 199–218.

Stern Y, Arenaza-Urquijo EM, Bartrés-Faz D, Belleville S, Cantilon M, Chetelat G, Ewers M, Franzmeier N, Kempermann G, Kremen WS, et al. Whitepaper: defining and investigating cognitive reserve, brain reserve, and brain maintenance. *Alzheimers Dement J Alzheimers Assoc*. 2020:16:1305–1311.

Tustison NJ, Avants BB, Cook PA, Zheng Y, Egan A, Yushkevich PA, Gee JC. N4ITK: improved N3 bias correction. *IEEE Trans Med Imaging*. 2010:29:1310–1320.

Vidal-Piñeiro D, Valls-Pedret C, Fernández-Cabello S, Arenaza-Urquijo EM, Sala-Llonch R, Solana E, Bargalló N, Junqué C, Ros E, Bartrés-Faz D. Decreased default mode network connectivity correlates with age-associated structural and cognitive changes. *Front Aging Neurosci*. 2014:6:256.

Vidal-Piñeiro D, Sneve MH, Storsve AB, Roe JM, Walhovd KB, Fjell AM. Neural correlates of durable memories across the adult lifespan: brain activity at encoding and retrieval. *Neurobiol Aging*. 2017:60:20–33.

Vidal-Piñeiro D, Sneve MH, Nyberg LH, Mowinckel AM, Sederevicius D, Walhovd KB, Fjell AM. Maintained frontal activity underlies high memory function over 8 years in aging. *Cereb Cortex*. 2019:29:3111–3123.

Viladomat J, Mazumder R, McInturff A, McCauley DJ, Hastie T. Assessing the significance of global and local correlations under spatial autocorrelation: a nonparametric approach. *Biometrics*. 2014:70:409–418.

Wager TD, Lindquist MA, Nichols TE, Kober H, Van Snellenberg JX. Evaluating the consistency and specificity of neuroimaging data using meta-analysis. *NeuroImage*. 2009:45:S210–S221.

Wang L, Li Y, Metzak P, He Y, Woodward TS. Age-related changes in topological patterns of large-scale brain functional networks during memory encoding and recognition. *NeuroImage*. 2010:50:862–872.

Wechsler T. *Wechsler abbreviated scale of intelligence*. San Antonio, TX: Psychological Corporation (PsychCorp); 1999

Xia M, Wang J, He Y. BrainNet viewer: a network visualization tool for human brain connectomics. *PLoS One*. 2013:8:e68910.

Yarkoni T, Poldrack RA, Nichols TE, Van Essen DC, Wager TD. Large-scale automated synthesis of human functional neuroimaging data. *Nat Methods*. 2011:8:665–670.

Yeo BTT, Krienen FM, Sepulcre J, Sabuncu MR, Lashkari D, Hollinshead M, Roffman JL, Smoller JW, Zöllei L, Polimeni JR, et al. The organization of the human cerebral cortex estimated by intrinsic functional connectivity. *J Neurophysiol*. 2011:106:1125–1165.

Zalesky A, Fornito A, Bullmore ET. Network-based statistic: identifying differences in brain networks. *NeuroImage*. 2010:53:1197–1207.

Zhang Y, Brady M, Smith S. Segmentation of brain MR images through a hidden Markov random field model and the expectation-maximization algorithm. *IEEE Trans Med Imaging*. 2001:20:45–57.